Quasiparticle band structure of infinite hydrogen fluoride and hydrogen chloride chains

Christian Buth*

Max-Planck-Institut für Physik komplexer Systeme, Nöthnitzer Straße 38, 01187 Dresden, Germany

(Dated: June 2, 2006)

I study the quasiparticle band structure of isolated, infinite $(HF)_\infty$ and $(HCl)_\infty$ bent (zig-zag) chains and examine the effect of the crystal field on the energy levels of the constituent monomers. The chains are one of the simplest but realistic models of the corresponding three-dimensional crystalline solids. To describe the isolated monomers and the chains, I set out from the Hartree-Fock approximation, harnessing the advanced Green's function methods *local molecular orbital algebraic diagrammatic construction scheme* (ADC) and *local crystal orbital ADC* (CO-ADC) in a strict second order approximation, ADC(2,2) and CO-ADC(2,2), respectively, to account for electron correlations. The configuration space of the periodic correlation calculations is found to converge rapidly only requiring nearest neighbor contributions to be regarded. Although electron correlations cause a pronounced shift of the quasiparticle band structure of the chains, with respect to the Hartree-Fock result, the band width essentially remains unaltered in contrast to, e.g., covalently bound compounds.

PACS numbers: 71.20.-b, 71.15.Qe, 71.20.Ps, 31.15.Ar

I. INTRODUCTION

Hydrogen fluoride[1,2,3,4,5] and hydrogen chloride[6,7] are representatives of hydrogen-bonded crystals. This type of bonding[8,9,10,11,12] is weak and essentially preserves the electronic structure of the constituent HF and HCl monomers, respectively. Hydrogen fluoride forms strong hydrogen bonds whereas hydrogen chloride forms only weak hydrogen bonds. Therefore, they are good candidates to study the quasiparticle band structure of hydrogen-bonded periodic systems. The structure of both crystals is very similar at low temperatures; the monomers are arranged in terms of weakly interacting parallel zig-zag chains. The isolated infinite chain is considered to be a simple but realistic one-dimensional model for the three-dimensional crystals.[13,14,15,16,17,18,19,20,21]

The isolated $(HF)_\infty$ and $(HCl)_\infty$ chains have been studied carefully; particularly the ground state has been examined,[13,14,15,16,17,18,19,20,21] e.g., Refs. 19,20,21 give a detailed *ab initio* analysis of the electron correlation contributions and the basis set dependence of the binding energy. The Hartree-Fock band structure of $(HF)_\infty$ is discussed in Refs. 13,14,16,17,20,22 and the one of the $(HCl)_\infty$ chain is investigated in Refs. 13,14,15,18. Correlation corrections for $(HF)_\infty$ have been obtained for the center (Γ-point) and the edge (X-point) of the Brillouin zone by Liegener and Ladik[16] who employed outer valence Green's functions (OVGFs).[23,24,25,26] No correlation corrections have been determined for $(HCl)_\infty$ so far.

To carry out accurate *ab initio* correlation calculations for periodic systems, I set out from the WANNIER program[27,28] which directly produces Wannier orbitals by solving modified Hartree-Fock equations.[20,29] To account for electron correlations, an advanced Green's function method, the crystal orbital algebraic diagrammatic construction scheme (CO-ADC) for Wannier orbitals[20,30] is

used. It has been devised recently on the basis of the well-established ADC scheme for atoms, molecules, and clusters.[31,32] It is a method to approximate the Feynman-Dyson perturbation series for the self-energy and contains sums of certain proper and improper diagrams to infinite order. The scheme sets out from the equations in terms of Bloch orbitals[20,30,33] and expresses them in Wannier representation which allows to specify efficient cut off criteria for the configuration space. The well-known robustness of the ADC method even facilitates to study strong electron correlations which typically occur when inner valence electrons are treated.[34,35] Yet in this work, I focus on the quasiparticle (or main) states for which a one to one correspondence to Hartree-Fock one-particle states can be established. Like the one-particle states, they form a so-called quasiparticle band structure.[36,37] The CO-ADC theory[20,30] has been implemented on top of WANNIER in terms of the CO-ADC program.[38]

This article is structured as follows: the ADC and CO-ADC schemes in local representation are introduced in Sec. II whereas Sec. III describes geometries, basis sets, cutoffs, and the computer programs employed. I devote Sec. IV to the discussion of the energy levels of the HF and HCl monomers paying particularly attention to the impact of electron correlations and their implications. The quasiparticle band structure of the infinite chains is investigated in Sec. V. Conclusions are drawn in Sec. VI.

II. THEORY

In order to determine the energy levels of atoms, molecules, clusters, or crystals theoretically, I set out from the Schrödinger equation with the full non-relativistic Hamiltonian neglecting nuclear motions; the ground state is obtained in restricted, closed-shell Hartree-Fock approximation.[25,26,36,39,40,41] From the or-

bital energies, the ionization potentials (IPs) and electron affinities (EAs) follow immediately by Koopmans' theorem;[42,43,44] the energy levels are simply given by their negative value, i.e., -IP and -EA.

Taking electron correlations into account, the energy levels now result from the poles of the one-particle Green's function (or particle propagator)[32,40,45,46,47] in energy representation; it is expressed using atomic units in the spectral or Lehmann representation by[45,46,47]

$$
G_{pq}(\vec{k}, \omega) = \sum_{n \in \{N+1\}} \frac{y_p^{(n)}(\vec{k}) \, y_q^{(n)*}(\vec{k})}{\omega + A_n(\vec{k}) + i\eta} \\
+ \sum_{n \in \{N-1\}} \frac{x_p^{(n)}(\vec{k}) \, x_q^{(n)*}(\vec{k})}{\omega + I_n(\vec{k}) - i\eta}
\tag{1}
$$

and depends on the crystal momentum $\vec{k}$. The residue amplitudes are $y_p^{(n)}(\vec{k}) = \langle \Psi_0^N | \hat{c}_{\vec{k}\,p} | \Psi_n^{N+1}(\vec{k}) \rangle$ and $x_p^{(n)}(\vec{k}) = \langle \Psi_n^{N-1}(-\vec{k}) | \hat{c}_{\vec{k}\,p} | \Psi_0^N \rangle$ where $\hat{c}_{\vec{k}\,p}$ and $\hat{c}_{\vec{k}\,p}^\dagger$ destroy and create, respectively, electrons in the Hartree-Fock Bloch orbital $\psi_{\vec{k}\,p}(\vec{r}\,s)$. Here $\vec{r}$ and s correspondingly denote spatial and spin coordinates. The negative value of the pole positions of $G_{pq}(\vec{k}, \omega)$ are the IPs and the EAs, $I_n(\vec{k})$ and $A_n(\vec{k})$, respectively. The infinitesimal $\eta > 0$ in Eq. (1) is needed to render the Fourier transformation between time and energy variables convergent.

The pole strengths or spectroscopic factors are defined by[23] $|x_p^{(n)}(\vec{k})|^2$ and $|y_p^{(n)}(\vec{k})|^2$ for IPs and EAs, correspondingly. Summing over all Bloch orbitals yields the orbital independent pole strengths which are given by[48]

$$
\begin{aligned}
P_+^{(n)} &= \sum_{\vec{k}\,p} |y_p^{(n)}(\vec{k})|^2 \\
P_-^{(n)} &= \sum_{\vec{k}\,p} |x_p^{(n)}(\vec{k})|^2 .
\end{aligned}
\tag{2}
$$

The inequalities $0 \leq |y_p^{(n)}(\vec{k})|^2, |x_p^{(n)}(\vec{k})|^2, P_\pm^{(n)} \leq 1$ hold. As $P_\pm^{(n)} = 1$ for the nth IP and EA, respectively, obtained in Hartree-Fock approximation via Koopmans theorem,[42,43,44] formula (2) also is a measure of the one-particle character of the nth state. Moreover, the pole strengths quantify the relative spectral intensities measured in (inverse) photoelectron experiments.[23]

To evaluate the particle propagator (1), the self-energy $\Sigma_{rs}(\vec{k}, \omega)$ with respect to the residual interaction—here the difference between the full Hamiltonian and the Fock operator—is introduced via the Dyson equation[32,40,45,46,47]

$$
\boldsymbol{G}(\vec{k}, \omega) = \boldsymbol{G}^0(\vec{k}, \omega) + \boldsymbol{G}^0(\vec{k}, \omega)\, \boldsymbol{\Sigma}(\vec{k}, \omega)\, \boldsymbol{G}(\vec{k}, \omega) , \tag{3}
$$

where $G_{pq}^0(\vec{k}, \omega)$ denotes the Green's function of the non-interacting system. The self-energy naturally decomposes into an energy independent part, the static self-energy, and an energy dependent part, the dynamic self-energy,[23,32]

$$
\boldsymbol{\Sigma}(\vec{k}, \omega) = \boldsymbol{\Sigma}^\infty(\vec{k}) + \boldsymbol{M}(\vec{k}, \omega) \tag{4}
$$

with $\lim_{\omega \to \pm\infty} \boldsymbol{M}(\vec{k}, \omega) = \boldsymbol{0}$. The dynamic self-energy also breaks down into two contributions

$$
\boldsymbol{M}(\vec{k}, \omega) = \boldsymbol{M}^+(\vec{k}, \omega) + \boldsymbol{M}^-(\vec{k}, \omega) . \tag{5}
$$

The static and the dynamic self-energy are related by[20,23,30,49,50]

$$
\Sigma_{pq}^\infty(\vec{k}) = \sum_{\vec{k}'} \sum_{r,s} V_{\vec{k}\,p\,\vec{k}'\,r\,[\vec{k}\,q\,\vec{k}'\,s]} \Big[\frac{1}{2\pi i} \oint \sum_{u,v} G_{su}^0(\vec{k}', \omega) \\
\times (\Sigma_{uv}^\infty(\vec{k}', \omega) + M_{uv}(\vec{k}', \omega))\, G_{vr}(\vec{k}', \omega)\, d\omega \Big] .
\tag{6}
$$

Here $V_{\vec{k}\,p\,\vec{k}'\,r\,[\vec{k}\,q\,\vec{k}'\,s]}$ are antisymmetrized two-electron integrals[20,30,42,43,44] and the contour integration runs along the real axis and closes in the upper complex ω-plane.[23,49,50] Formula (6) can be evaluated using the Dyson expansion method (DEM).[20,30,49] Due to this relation, it is sufficient to concentrate on the approximation of the dynamic self-energy because the static part can be obtained from it afterwards.

The algebraic diagrammatic construction scheme is used to express the dynamic self-energy in a non-diagonal representation

$$
M_{rs}^\pm(\vec{k}, \omega) = \vec{U}_r^{\pm\dagger}(\vec{k})\, (\omega \, \mathbb{1} - \boldsymbol{K}^\pm(\vec{k}) - \boldsymbol{C}^\pm(\vec{k}))^{-1}\, \vec{U}_s^\pm(\vec{k}) ,
\tag{7}
$$

the so-called general algebraic form or ADC form. The nth order approximation of the ADC is constructed by inserting the perturbation ansatz in terms of the residual interaction $\boldsymbol{U}^\pm(\vec{k}) = \boldsymbol{U}^{\pm(1)}(\vec{k}) + \boldsymbol{U}^{\pm(2)}(\vec{k}) + \ldots$ and $\boldsymbol{C}^\pm(\vec{k}) = \boldsymbol{C}^{\pm(1)}(\vec{k}) + \boldsymbol{C}^{\pm(2)}(\vec{k}) + \ldots$, into Eq. (7) and expanding the resulting formula into a geometric series.[20,30,32] Comparing the resulting terms with the terms arising in the Feynman-Dyson perturbation expansion, analytical expressions can be found for the matrices showing up in Eq. (7). Thereby, frequently linear combinations of the expressions of a few diagrams have to be formed. The construction works because both series have the same analytic structure.

To evaluate the dynamic self-energy in Eq. (7), I switch to a representation in terms of generalized Wannier orbitals. Such a local representation is particularly beneficial to treat crystals with a large unit cell.[20,25,26,30,36,37] Suitable schemes to express the crystal momentum dependent ADC form (7) using Wannier orbitals are discussed in Refs. 20,30. In this work, I exclusively use the fully translational symmetry adapted form in Eq. (29) of Ref. 30.

When changing to Wannier orbitals, one has to keep in mind that the Fock matrix is no longer diagonal. The off-diagonal matrix elements are most efficiently accounted for by a diagrammatic expansion in addition to the perturbative evaluation of the two-electron interaction.[20,30] The resulting approximation schemes are denoted by CO-ADC(m,n). This notation indicates that the contributions which (partly) involve one-electron interactions are treated in order m and the contributions that are exclusively given by two-electron interactions are treated in

order n. In this article, I resort to the lowest order CO-ADC(2,2) approximation in Eq. (32) of Ref. 30. Then, in Eq. (5) of this work, $M_{rs}^+(\vec{k}, \omega)$ is associated with two-particle-one-hole ($2p1h$) configurations and $M_{rs}^-(\vec{k}, \omega)$ involves two-hole-one-particle ($2h1p$) configurations.[20,30]

Having explicit expressions for the translational symmetry adapted Fock matrix $\boldsymbol{F}(\vec{k})$ and the static and the dynamic self-energy, the energy levels of a crystal can be determined for the crystal momenta $\vec{k}$; they are given by the eigenvalues $\boldsymbol{E}(\vec{k})$ of the Hermitian band structure matrix

$$
\boldsymbol{B}(\vec{k}) = \begin{pmatrix} \boldsymbol{F}(\vec{k}) + \boldsymbol{\Sigma}^\infty(\vec{k}) & \boldsymbol{U}^{+\dagger}(\vec{k}) & \boldsymbol{U}^{-\dagger}(\vec{k}) \\ \boldsymbol{U}^+(\vec{k}) & \boldsymbol{K}^+(\vec{k}) + \boldsymbol{C}^+(\vec{k}) & \boldsymbol{0} \\ \boldsymbol{U}^-(\vec{k}) & \boldsymbol{0} & \boldsymbol{K}^-(\vec{k}) + \boldsymbol{C}^-(\vec{k}) \end{pmatrix} , \tag{8}
$$

which are obtained by solving the eigenvalue problem

$$
\boldsymbol{B}(\vec{k})\boldsymbol{X}(\vec{k}) = \boldsymbol{X}(\vec{k})\boldsymbol{E}(\vec{k}), \qquad \boldsymbol{X}^\dagger(\vec{k})\,\boldsymbol{X}(\vec{k}) = \mathbb{1} . \tag{9}
$$

Here $\boldsymbol{X}(\vec{k})$ denotes the eigenvectors of $\boldsymbol{B}(\vec{k})$. Its matrix elements, $X_{pn}(\vec{k})$, represent the residual amplitudes $y_p^{(n)}(\vec{k})$ or $x_p^{(n)}(\vec{k})$ in Eq. (2) depending on whether they are of $N+1$ or of $N-1$ type.

As crystals are infinite, the lattice sums occurring in the expressions for $\boldsymbol{B}(\vec{k})$ have to be truncated using a suitable cutoff procedure. Furthermore, the configuration space, i.e., the number of $2p1h$- and $2h1p$-configurations considered to form $\boldsymbol{B}(\vec{k})$ needs to be restricted.[20,30] Both goals can be met by realizing that the importance of individual configurations for the description of the energy levels of a crystal can be measured by the magnitude of the one- and the two-electron integrals involved. This criterion allows a very fine grained, individual selection of configurations according to a given cutoff threshold. This procedure is termed configuration selection; it can be shown to converge with the distance from the origin cell of the Wannier orbitals constituting the configurations.[20,30]

Having set up the band structure matrix, its partial diagonalization is carried out efficiently using a complex-Hermitian band-(or block-)Lanczos algorithm.[20,30] The computer code is based on the complex-symmetric version of Sommerfeld[51] that, in turn, is an adaption of the real-symmetric implementation by Meyer.[51] Band Lanczos methods are iterative algorithms that utilize the product of a matrix, here $\boldsymbol{B}(\vec{k})$, with a few vectors to transform the original matrix into a band diagonal form which subsequently can be diagonalized efficiently.[50,52,53] The band-Lanczos algorithm usually converges to the spectral envelope already after a few matrix times vector operations. This corresponds to only moderately sized band diagonal matrices.[50,52]

A quasiparticle point of view is assumed for the outer valence regime and the lowest virtual states, i.e., I focus on those states which are essentially of one-particle character with only a moderate adjustment due to electron correlations.[36,37] The number of quasiparticle bands is the same as the number of Hartree-Fock bands and a clear association between both can be made. To identify the quasiparticle states of a crystal in the spectrum of $\boldsymbol{B}(\vec{k})$, I resort to the orbital independent pole strength (2) extracting only states with $P_\pm^{(n)} > 0.7$. In analogy to the energies of one-particle states, the quasiparticle energy levels group into bands with respect to the crystal momentum forming a so-called quasiparticle band structure.

A local orbital based ADC scheme for isolated molecules can easily be devised setting out from the CO-ADC equations in Wannier representation:[20,30] let the unit cell of a primitive cubic crystal lattice with a macroscopic lattice constant be occupied by a given molecule. Then only Fock matrix elements and two-electron integrals within a unit cell are non-negligible. Consequently, all states of the crystal are N_0 fold degenerate and the band structure matrix has only to be diagonalized at the Γ point to obtain all distinct energy levels of the crystal.[20,30] These levels can be identified with the energy levels of the isolated molecule. By this line of argument, it is justified to drop the lattice sums and lattice vectors totally in the CO-ADC equations to obtain analytical expressions for the local molecular orbital ADC scheme. The dependence on the crystal momentum quantum number vanishes and the resulting matrix $\boldsymbol{B}$ is now termed energy level matrix. Similarly to the nomenclature for the methods based on crystal orbital ADC, the corresponding approximative schemes for molecules are referred to as ADC(m,n).

III. COMPUTATIONAL DETAILS

Hydrogen fluoride and hydrogen chloride monomers are diatomic molecules of $C_{\infty v}$ symmetry. The experimental value for the internuclear distance is $0.91680\,\text{Å}$ for HF and $1.27455\,\text{Å}$ for HCl.[54] Upon crystallization to a three-dimensional solid, the HF and HCl monomers arrange in long zig-zag chains. The structure of the single
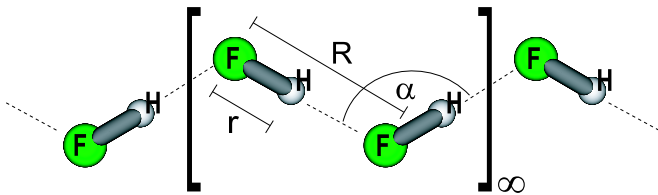
FIG. 1: (Color online) Structure of the infinite $(HF)_\infty$ zig-zag chain. The structure of $(HCl)_\infty$ is analogous.

FIG. 2: (Color online) Ionization potentials and electron affinities of a HF and a HCl molecule where IP > 0 and EA < 0. Solid green lines denote Hartree-Fock values (Koopmans' theorem[42,43,44]); dashed red lines depict ADC(2,2) results.

infinite $(HF)_\infty$ and $(HCl)_\infty$ chain [Fig. 1] is determined by three parameters, the H—X distance r, the X$\cdots$X distance R and the angle $\alpha = \angle(HXH)$ with X = F,Cl. The following experimental values for the parameters are taken: $r = 0.92$ Å, $R = 2.50$ Å, and $\alpha = 120°$ for $(HF)_\infty$[1,55] and $r = 1.25$ Å, $R = 3.688$ Å, and $\alpha = 93.3°$ for $(DCl)_\infty$.[6] Structural information for HCl crystals are not available. Yet HCl and DCl crystals have very similar lattice constants and are considered to be isomorphous.[6] Furthermore, I use the cc-pVDZ basis set[56,57,58] to represent H, F and Cl atoms in the compounds.[72]

A self-consistent solution of the Hartree-Fock equations is carried out with the WANNIER program[27,28] which directly yields Wannier orbitals.[20,29] A finite cluster of unit cells is utilized by WANNIER serving as a support for the Wannier orbitals in the origin cell. It consists of the origin cell and up to fourth nearest neighbor cells (nine unit cells altogether) for $(HF)_\infty$ and up to third nearest neighbor cells (seven unit cells altogether) for the $(HCl)_\infty$ chain. To carry out Hartree-Fock calculations for molecules, I let each unit cell of a one-dimensional lattice with a constant of $1\,\mu$m comprise a monomer. This ensures that interactions with neighboring unit cells, which contain periodic images of the molecule, are negligible. The Wannier orbitals in the origin cell can thus be identified with the orbitals of the isolated monomer.

As WANNIER determines only occupied Wannier orbitals, translationally related projected atomic orbitals, so-called crystal projected atomic orbitals,[20,59] have been devised to be used as virtual Wannier orbitals.[73] They are based on of the projected atomic orbitals introduced by Pulay and Saebø[60,61] and implemented by Hampel et al..[62,63] The WANNIER program produces pseudocanonical Wannier orbitals, i.e., the occupied block of the Fock matrix in the origin cell is diagonalized. Therefore, in the case of molecules occupying a primitive cubic crystal with a macroscopic lattice constant, only the virtual block in terms of the projected atomic orbitals[20,59] contains off-diagonal matrix elements.

The WANNIER program[27,28] also performs the transformation of the Fock matrix elements and the two-electron integrals from a representation in terms of one-particle basis functions to the Wannier representation. These quantities are the only ones which enter subsequent correlation calculations by the local molecular orbital ADC and the local crystal orbital ADC methods. In this study, I apply the lowest order approximation,
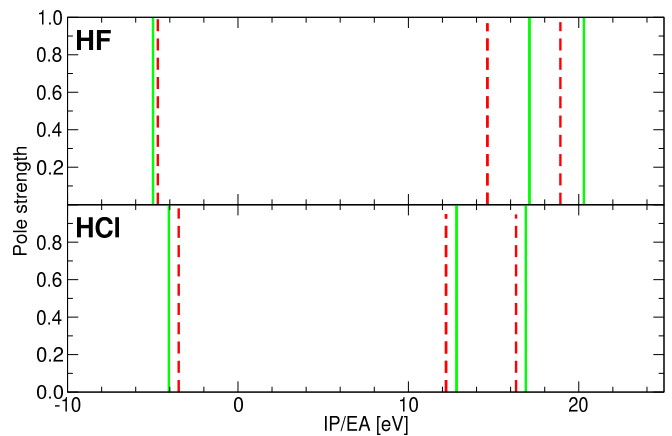
ADC(2,2) and CO-ADC(2,2) to molecules and infinite chains, respectively. To this end, I remove the explicit spin-dependence of the equations involved, following the arguments of Niessen et al..[24] The resulting equations for the two methods are implemented in terms of the CO-ADC program.[38]

Both ADC(2,2) and CO-ADC(2,2) employ an additional perturbative expansion of the off-diagonal terms of the Fock matrix in local orbitals with respect to their canonical orbital based counterparts. This introduces an extra approximation using ADC(2,2) in relation to ADC(2) whose accuracy has been critically assessed in Ref. 20 for the case of a single HF molecule. The outer valence IPs and the smallest EAs are found to be well-described by the correlation method. Yet it is not able to accurately describe the strong electron correlations which are observed in the inner valence region (F $2s$ dominated states) of the HF monomer.[20] This limitation of the method does not imply a constraint for this work because I focus exclusively on the main states of the systems.

IV. HF AND HCl MONOMERS

Before I turn to the infinite chains in Sec. V, I investigate the ionization potentials (IPs) and the electron affinities (EAs) of isolated diatomic HF and HCl monomers. This will allow to better interpret the band structures of the chains later on. On the abscissa of Fig. 2, I give the IPs (≥ 0) and EAs (< 0) of the molecules while the ordinate indicates the pole strength, Eq. (2), of each state. Numerical values are listed in Tabs. I and II. I do not present data which corresponds to the IPs of F $1s$ type core states and F $2s$ type inner valence states for HF. Neither do I show the core states of Cl $1s$, Cl $2s$,

Level No.	$-\varepsilon$	IP$_{2,2}$/EA$_{2,2}$	IP$_3$
3	20.30	18.92	20.32
4, 5	17.11	14.64	16.55
6	-4.99	-4.70	

TABLE I: Ionization potentials and electron affinities of a HF molecule. They are given in Hartree-Fock approximation by the negative value of the orbital energies $-\varepsilon$; the ADC(2,2) values are denoted by IP$_{2,2}$/EA$_{2,2}$. The very precise nD-ADC(3) results of Ref. 65, IP$_3$, which were determined with the aug-cc-pVTZ basis set are given as reference values. All data are given in electronvolts.

Level No.	$-\varepsilon$	IP$_{2,2}$/EA$_{2,2}$	IP$_4$
7	16.89	16.32	16.43
8, 9	12.83	12.21	12.41
10	-4.06	-3.48	

TABLE II: Ionization potentials and electron affinities of a HCl molecule. Symbols are chosen as in Tab. I where the reference values are given this time by IP$_4$; they were obtained in Ref. 48 using a simplified ADC(4) scheme together with basis set I. All data are given in electronvolts.

and Cl $3s$ type in conjunction with the inner valence states of Cl $2p$ origin for HCl. Above all, only the EA with the lowest energy in the given basis set is displayed. Yet the resonance properties[64] of the molecules are not investigated here further. The data are obtained in two different ways; once directly from the Hartree-Fock orbital energies by exploiting Koopmans' theorem[42,43,44] and the other time in ADC(2,2) approximation. The good accuracy of the ADC(2,2) results is corroborated by a comparison with the IPs which were obtained with higher order approximations of the theory in Tabs. I and II.

Many of the characteristics of the IPs and the EAs of the two molecules can already be understood in the independent particle model. The outer valence region of the two molecules is formed by two distinct IPs in the range of 15–20 eV for HF and of 10–20 eV for HCl. By inspecting the molecular orbitals, I find the lowest IPs of both monomers to correspond to an ionization from the two equivalent π-type lone pairs on fluorine and chlorine, respectively; consequently, they are twofold degenerate. Ionization from the third σ-type pair requires more energy as it is oriented towards the hydrogen atom and thus is attracted by its positive partial charge.

In the two spectra, the differences between fluorine and chlorine atoms basically manifest themselves in three effects. Firstly, there is an overall shift of all IPs and EAs of HCl to lower energies with respect to corresponding IPs in HF because in chlorine the nuclear charge is shielded by the lower lying Cl $2s$ and Cl $2p$ shells which are missing in the fluorine atom.[74] Secondly, the larger internuclear distance in HCl results in a weaker interaction between hydrogen and chlorine atoms compared with the interaction between hydrogen and fluorine atoms. Thirdly, the lower electronegativity of the chlorine atom causes HCl to be more covalently bonded than HF; it leads to the observed larger splitting of the outer valence IPs for HCl.

The IPs and EAs of HF and HCl change considerably as soon as one accounts for electron correlations; they shift substantially to lower energies with respect to the corresponding Hartree-Fock values.[36] The displacement of the IPs in the outer valence region is noticeably smaller for HCl compared with HF; the contrary holds for the

lowest EA. Generally, the Hartree-Fock IPs and EAs are more accurate for HCl than for HF which leads to the conclusion that electron correlations are less important for these states of HCl. This finding can be ascribed to the fact that the chlorine atom is notably bigger than the fluorine atom. Hence, the valence electrons of HF are squeezed to a smaller volume leading to a worse performance of Hartree-Fock theory; it is caused by an insufficient description of the Coulomb hole around the electrons which is especially important in the case of large geometrical orbital overlaps.[36,42,43,44] The energy splitting of the IPs of HF is slightly increased with respect to the Hartree-Fock result whereas it remains nearly the same for HCl. Moreover, the approximately uniform shift of the outer valence IPs of HF and HCl indicates that electron correlations for these states are dominated by the fluorine and the chlorine atom, respectively, and are essentially unaltered upon formation of the molecular bond.

V. HF AND HCl CHAINS

Having understood the nature of the IPs and EAs of the HF and HCl molecule in the previous Sec. IV, their changes upon crystallization can now be studied.

The Hartree-Fock band structure of the $(HF)_\infty$ and the $(HCl)_\infty$ chain is displayed in Figs. 3 and 4, respectively; a closeup of the valence bands is shown in Figs. 5 and 6. Numerical data of the energy levels of both compounds at the Γ and the X point are given in Tabs. III and IV.[75] As a unit cell of the chains comprises two monomers, the number of Hartree-Fock bands is twice the number of Hartree-Fock IPs and EAs of the monomer [Fig. 2 and Tabs. I and II]. For $(HF)_\infty$, the four low lying occupied bands, which mainly correspond to F $1s$ core states and F $2s$ inner valence states, are left out. Similarly, I do not show the energy bands originating from Cl $1s$, Cl $2s$, and Cl $2p$ core states and the inner valence of Cl $3s$ character. Furthermore, only the four lower conduction bands are given for both compounds. Again an examination of resonance properties[64] is not pursued further.

The Hartree-Fock bands which are situated energetically around -18 eV for $(HF)_\infty$ and around -12 eV for $(HCl)_\infty$ are formed by the two equivalent π-type
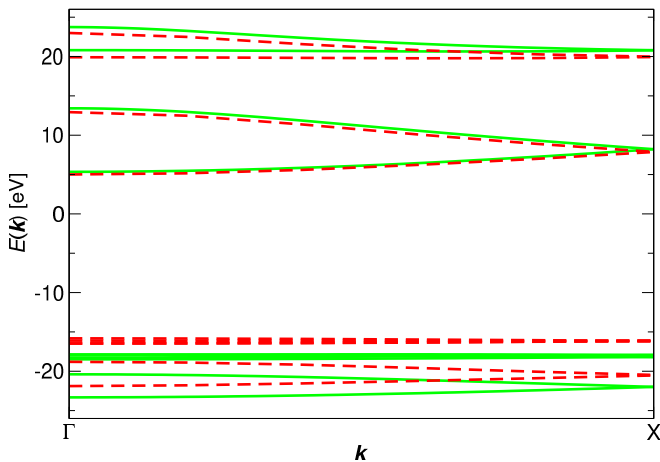
FIG. 3: (Color online) Band structure of a $(HF)_\infty$ chain. Hartree-Fock bands are given by solid green lines. The dashed red lines depict CO-ADC(2,2) quasiparticle bands which are determined by accounting for $2p1h$- and $2h1p$-configurations that involve Wannier orbitals in the origin cell, the nearest and the next nearest-neighbor cells.

lone pairs of mostly F $2p$ and Cl $3p$ character of the isolated molecules at -17.11 eV and -12.83 eV, respectively [Fig. 2 and Tabs. I and II]. Note that -IP or -EA, correspondingly, give the energy level. By inspection of Fig. 3, I see that the degeneracy of the molecular orbitals is lifted only slightly due to the crystal field upon formation of the infinite chain. The lowest valence bands cross in Figs. 5 and 6, which is allowed by rod group symmetry.

The energy bands of $(HF)_\infty$ in the range -24 eV to -20 eV and of $(HCl)_\infty$ between -18 eV to -17 eV are constituted by the third outer valence orbital of the isolated monomers which is also predominantly of F $2p$ and Cl $3p$ character with an orbital energy of -20.30 eV and of -16.89 eV, respectively [Fig. 2 and Tabs. I and II]. The dispersion of these two energy bands is much larger than the dispersion of the four bands discussed in the previous paragraph. This indicates that hydrogen bonding in the chains is mainly mediated by the orbitals of the monomers which lead to these two outer valence bands.

The Hartree-Fock band structure of the $(HF)_\infty$ chain is reported by Berski and Latajka[17] for a series of basis sets. Among these, the 6-31+G(d,p) basis is of most comparable quality to the cc-pVDZ basis[56,58] employed in this study; the plot of the band structure of $(HF)_\infty$ in Fig. 3 of Ref. 17 agrees very well with the plot in Fig. 5 of this article. I read off the energy of the top of the valence bands at the Γ point from Fig. 3 of Berski and Latajka;[17] it lies at -18.3 eV which is very close to my value of -17.9 eV from Tab. V. The Hartree-Fock band structure of the $(HF)_\infty$ chain has also been studied by Liegener and Ladik[16] who use a double-ζ basis set $[(9s\,5p)\,/\,[3s\,2p]$ for fluorine and $(6s\,1p)\,/\,[2s\,1p]$ for hydrogen to which they refer as DZP basis set. They observe that unit cells up to third nearest neighbors are sufficient to represent the Fock matrix. My computa-
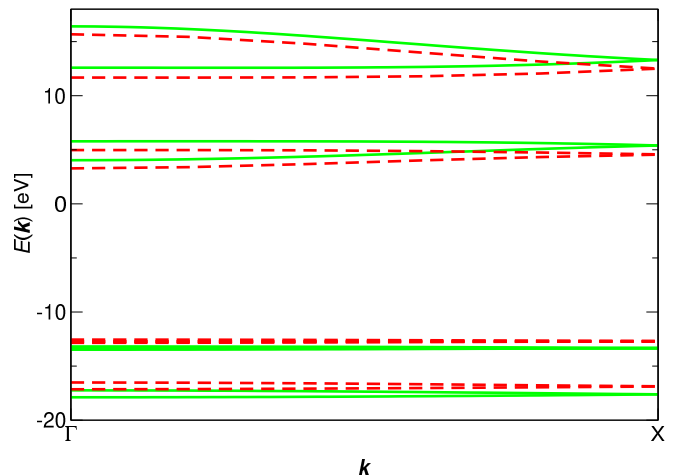

FIG. 4: (Color online) Band structure of a $(HCl)_\infty$ chain. Symbols are chosen as in Fig. 3.

tions confirm this finding. Liegener and Ladik[16] obtain an energy of -17.57 eV for the top of the valence bands and 3.57 eV for the bottom of the conduction bands, i.e., their Hartree-Fock band gap amounts to 21.14 eV. The top of the valence bands is only by 0.3 eV smaller than my result at the Γ point. However, the bottom of the conduction bands is by 1.78 eV smaller than mine. The deviation of my result from those of Liegener and Ladik[16] can most likely be ascribed to the different basis sets employed, i.e., cc-pVDZ versus DZP because the DZP basis set lacks a d-function on fluorine which is present for cc-pVDZ.[56,58]

Blumen and Merkel[15] treat the $(HCl)_\infty$ chain using a $(3s)\,/\,[1s]$ basis on hydrogen and a $(10s\,6p)\,/\,[3s\,2p]$ basis on chlorine. They include up to second nearest neighbor cells to represent the Fock matrix. Their band structure [Fig. 1 in Ref. 15] agrees nicely with Fig. 4 in this work. I read off the figure of Blumen and Merkel the value -13.4 eV for the top of the valence bands and 6.9 eV for the bottom of the conduction bands at the Γ point, yielding a band gap of 20.3 eV. My corresponding values are -13.186 eV and 4.035 eV [Tab. VI] amounting to a band gap of 17.221 eV which is somewhat smaller than the value of Blumen and Merkel. Again this can most likely be ascribed to the difference in the one-particle basis sets.

In order to investigate the effect of electron correlations on the band structures of the chains, I utilize the CO-ADC(2,2) method.[20,30] The convergence of several key quantities with respect to the number of unit cells whose Wannier orbitals are considered to form $2p1h$- and $2h1p$-configurations in correlation calculations are summarized in Tabs. V and VI for $(HF)_\infty$ and $(HCl)_\infty$, respectively. Namely, the top of the valence bands, the bottom of the conduction bands, the band gap and the width of the upper and the lower valence band complexes are shown. They are compared with the plain Hartree-Fock data (with "0" unit cells for the configuration selec-
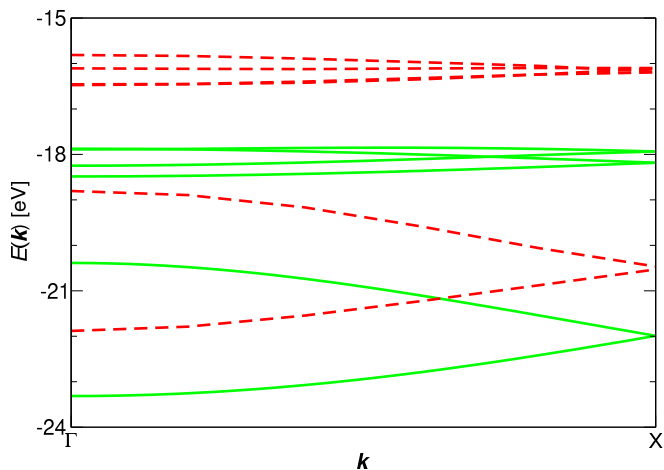
FIG. 5: (Color online) Valence band structure of a $(HF)_\infty$ chain. Zoom into Fig. 3.

FIG. 6: (Color online) Valence band structure of a $(HCl)_\infty$ chain. Zoom into Fig. 4.

tion). In first place, the quasiparticle band structure of the chains is obtained considering only a minimum fraction, a single unit cell, in correlation calculations.[76] This causes an upwards shift of the top of the valence bands by 1.90 eV for $(HF)_\infty$ and by 0.54 eV for $(HCl)_\infty$ whereas the bottom of the conduction bands shifts downwards by 0.22 eV for $(HF)_\infty$ and by 0.60 eV for $(HCl)_\infty$. Subsequently, I enlarge the configuration space to include also configurations which extend to the nearest-neighbor cells. This causes an additional shift of the top of the valence bands by 0.16 eV for $(HF)_\infty$ and by 0.10 eV for $(HCl)_\infty$. Moreover, a shift of the bottom of the conduction bands of 0.12 eV for $(HF)_\infty$ and of 0.15 eV for $(HCl)_\infty$ is observed. Further inclusion of second and third nearest-neighbor cells has only a minute effect. The other quantities in Tabs. V and VI exhibit a similarly quick convergence.

The fully converged quasiparticle band structures of the chains—configurations in up to second nearest-neighbor cells are considered—are shown aside of the Hartree-Fock band structures in Figs. 3 to 6. I observe pronounced corrections of the valence bands of $(HF)_\infty$ due to electron correlations. Their upwards shift is much larger than the downwards shift of the conduction bands. In $(HCl)_\infty$ the contrary holds, however, the value and the difference of the shifts is much smaller compared with $(HF)_\infty$. These observations match the behavior of the IPs and EAs found in the monomers in Sec. IV. There these trends are attributed to the larger compactness of the fluorine atom in relation to the chlorine atom. Moreover, an analysis of the ground-state binding energies of the chains shows a similar behavior of short-range contributions of electron correlations which are also significantly larger in $(HF)_\infty$ than in $(HCl)_\infty$.[19,20] Yet the impact of the configurations from more than a single unit cell in correlation calculations, were found to be bigger in $(HCl)_\infty$.

The observed long-range correlation corrections of the

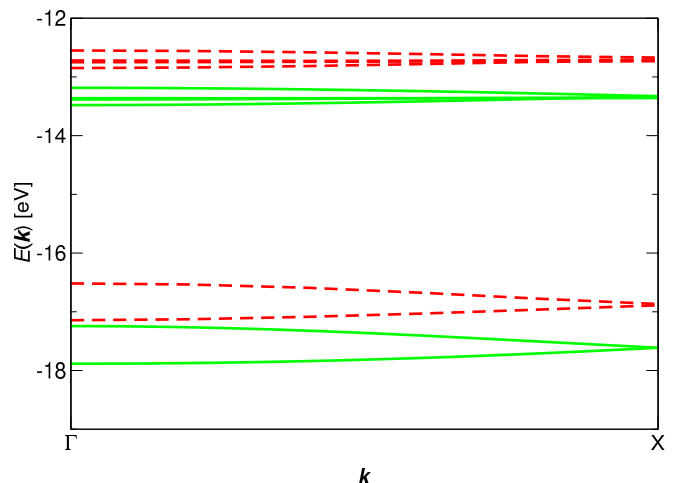quasiparticle band structures of the chains from more distant unit cells is, firstly, caused by the adjustment of the many-particle system to the extra charge of the electron which is added to or removed from it in the one-particle Green's function. Secondly, corrections due to van der Waals interactions take effect.[36]

Valence and conduction bands of both compounds do not shift symmetrically, i.e., by the same amount, upwards or downwards [for numerical values see Tabs. V and VI and the discussion of the convergence of the CO-ADC(2,2) calculations above]. Instead, in $(HF)_\infty$, the valence bands show a much stronger influence due to electron correlations than the conduction bands. The reverse trend is observed for $(HCl)_\infty$. However, the inclusion of nearest-neighbor cells in correlation calculations leads to essentially the same displacement of both types of bands, i.e., the assumption of a symmetric shift becomes valid for long-range contributions as pointed out in Ref. 66.

Although the quasiparticle bands are shifted appreciably with respect to the corresponding Hartree-Fock bands, they essentially maintain their shape. This observation is in contrast to the pronounced reduction of bandwidths due to electron correlations which are typically found in covalently bonded polymers like *trans*-polyacetylene[67] and in covalently bonded crystals like diamond or silicon.[66,68,69]

To investigate the accuracy of the CO-ADC(2,2) method, I compare with theoretical results from outer valence Green's functions (OVGFs)[23,24,25,26] which have been applied by Liegener and Ladik[16] to the $(HF)_\infty$ chain employing the DZP basis set. For the top of the valence bands and the bottom of the conduction bands at the Γ point, they obtain -15.10 eV and 3.05 eV, respectively, in second order OVGFs and -15.09 eV and 3.03 eV in third order OVGFs. The latter two numbers correspond to an increase of the valence band energy by 2.48 eV and a lowering of the conduction band energy by 0.54 eV with respect to the Hartree-Fock result. In

Band No.	$\varepsilon(\Gamma)$	$E_{2,2}(\Gamma)$	$\varepsilon(X)$	$E_{2,2}(X)$
5	-23.31	-21.88	-22.00	-20.50
6	-20.39	-18.80	-22.00	-20.50
7	-18.49	-16.48	-18.18	-16.19
8	-18.25	-16.46	-18.18	-16.19
9	-17.89	-16.11	-17.94	-16.11
10	-17.88	-15.81	-17.94	-16.11
11	5.35	5.01	8.22	7.88
12	13.42	12.93	8.22	7.88

TABLE III: Energy levels of an infinite $(HF)_\infty$ chain at the Γ and the X point. Here $\varepsilon(\vec{k})$ represents the Hartree-Fock Bloch orbital energies and $E_{2,2}(\vec{k})$ gives the CO-ADC(2,2) energies for the crystal momenta with $\vec{k} = \Gamma, X$ which were determined accounting for an extension of the $2p1h$- and $2h1p$-configurations up to third nearest neighbor cells. All data are given in electronvolts.

Band No.	$\varepsilon(\Gamma)$	$E_{2,2}(\Gamma)$	$\varepsilon(X)$	$E_{2,2}(X)$
13	-17.88	-17.14	-17.61	-16.88
14	-17.24	-16.52	-17.61	-16.88
15	-13.48	-12.85	-13.36	-12.73
16	-13.39	-12.75	-13.36	-12.73
17	-13.36	-12.72	-13.33	-12.69
18	-13.19	-12.55	-13.33	-12.69
19	4.04	3.28	5.40	4.56
20	5.78	4.97	5.40	4.56

TABLE IV: Energy levels of an infinite $(HCl)_\infty$ chain at the Γ and the X point. Labels are chosen as in Tab. III. This time $2p1h$- and $2h1p$-configurations are being formed by the Wannier orbitals in up to second nearest neighbor cells. All data are given in electronvolts.

contrast, CO-ADC(2,2) yields at the Γ point an increase by 2.08 eV and a lowering by 0.33 eV. The overall agreement between CO-ADC(2,2) and OVGFs is satisfactory. The deviations between the data from both methods, as already found for the Hartree-Fock band structure, can again be attributed predominantly to basis set artifacts.

To the best of my knowledge no correlation calculations of the quasiparticle band structure of $(HCl)_\infty$ chains have been performed to date.

VI. CONCLUSION

This work deals with the quasiparticle band structure of infinite $(HF)_\infty$ and $(HCl)_\infty$ chains which are determined and compared with the energy levels of the constituting monomers.

The analysis begins with the examination of the compounds in Hartree-Fock approximation. The band structure of both chains turns out to be quite similar. However, the bands of $(HCl)_\infty$ are shifted towards the band gap with respect to the bands of $(HF)_\infty$ chains. By analyzing the ionization potentials and electron affinities of the monomers, the origin of the individual bands of the infinite chains is identified. The higher outer valence bands stem from the lone pairs on fluorine and chlorine, respectively, and the lower outer valence bands originate from the hydrogen bonding. The latter bands also exhibit less dispersion in $(HCl)_\infty$ compared with $(HF)_\infty$ due to the weaker bonding.

Electron correlation calculations are performed to determine accurate energy levels of the HF and HCl molecules and precise quasiparticle band structures of the $(HF)_\infty$ and $(HCl)_\infty$ chains. To this end, I use the *ab initio* Green's function theory crystal orbital algebraic diagrammatic construction for Wannier orbitals. The strict second order approximation of the off-diagonal Fock matrix elements and the two-electron contributions is applied which is dubbed CO-ADC(2,2) method.[20,30] Setting out from these equations, I make the transition to the corresponding method for molecules, termed ADC(2,2), by eliminating the lattice summations. The configuration space of the correlation calculations is found to converge rapidly; only nearest neighbor cells need to be regarded to determine the band gap of the chains within 0.008 eV of the value obtained in the largest calculations performed. The inclusion of correlation effects leads to a pronounced shift of the quasiparticle bands with respect to the Hartree-Fock result. They are noticeably larger in the HF monomer and the $(HF)_\infty$ chain compared with the chlorine compounds.

To assess the accuracy of the ADC(2,2) ionization potentials of the monomers, I compare with independently obtained theoretical data; a reassuring agreement is found. Furthermore, the quasiparticle energies for the $(HF)_\infty$ chain compare very well with data from outer valence Green's functions (OVGFs)[23,24,25,26] thus corroborating the accuracy of the CO-ADC(2,2) scheme. In contrast to many other compounds, e.g., covalently bound polymers[67] or crystals,[66,67,68,69] the band width of the chains does not decrease substantially due to correlation effects but increases slightly.

Building on top of this work, one should investigate carefully the lower lying, inner valence regime of the chains where intriguing many-particle effects are to be expected.[34,35] Particularly one should investigate strong electron correlations and intermolecular electronic decay processes[70] found recently in atomic and molecular clusters, including clusters of HF molecules.[71]

Cells	$E_{\text{top,v}}$	$E_{\text{bottom,c}}$	E_{gap}	$\Delta E^{<}_{\text{F}\,2p}$	$\Delta E^{>}_{\text{F}\,2p}$
0	-17.876	5.347	23.223	2.924	0.610
1	-15.975	5.129	21.104	2.993	0.654
3	-15.815	5.011	20.825	3.078	0.664
5	-15.813	5.006	20.819	3.078	0.664
7	-15.812	5.005	20.817	3.078	0.664

TABLE V: Convergence of the fundamental band gap E_{gap} and the bandwidth of the lower and the upper F $2p$ valence band complexes, $\Delta E^{<}_{\text{F}\,2p}$ and $\Delta E^{>}_{\text{F}\,2p}$, respectively, of a $(\text{HF})_{\infty}$ chain with respect to the number of unit cells used to determine the quasiparticle band structures. "Cells" designates the number of unit cells taken into account in CO-ADC(2,2) calculations where zero refers to the original Hartree-Fock results. Unity denotes the $2p1h$- and $2h1p$-configurations from the origin cell only in correlation calculations. Three, five and seven indicate the additional inclusion of nearest, second nearest and third nearest-neighbor cells, respectively. The top of the valence bands $E_{\text{top,v}}$ and the bottom of the conduction bands $E_{\text{bottom,c}}$ are both situated at the Γ point. All data are given in electronvolts.

Cells	$E_{\text{top,v}}$	$E_{\text{bottom,c}}$	E_{gap}	$\Delta E^{<}_{\text{Cl}\,3p}$	$\Delta E^{>}_{\text{Cl}\,3p}$
0	-13.186	4.035	17.221	0.641	0.294
1	-12.651	3.434	16.085	0.620	0.288
3	-12.554	3.280	15.834	0.627	0.299
5	-12.550	3.277	15.827	0.627	0.299

TABLE VI: Convergence of the fundamental band gap E_{gap} and the bandwidth of the lower and upper Cl$3p$ valence band complexes, $\Delta E^{<}_{\text{Cl}\,3p}$ and $\Delta E^{>}_{\text{Cl}\,3p}$, respectively, of a $(\text{HCl})_{\infty}$ chain with respect to the number of unit cells used to determine the quasiparticle band structures. Symbols are chosen as in Tab. V. All data are given in electronvolts.

[*] Present address: Argonne National Laboratory, 9700 South Cass Avenue, Argonne, IL 60439, USA; electronic address: Christian.Buth@web.de

[1] M. Atoji and W. N. Lipscomb, Acta. Cryst. **7**, 173 (1954).

[2] S. P. Habuda and Y. V. Gagarinsky, Acta. Cryst. **B27**, 1677 (1971).

[3] P. Otto and E. O. Steinborn, Solid State Communications **58**, 281 (1986).

[4] I. Panas, Int. J. Quantum Chem. **46**, 109 (1993).

[5] S. Berski and Z. Latajka, J. Mol. Struct. **450**, 259 (1998).

[6] E. Sándor and R. F. C. Farrow, Nature **213**, 171 (1967).

[7] E. Sándor and R. F. C. Farrow, Nature **215**, 1265 (1967).

[8] W. C. Hamilton and J. A. Ibers, *Hydrogen bonding in solids* (Benjamin, New York, Amsterdam, 1968).

[9] L. Pauling, *The nature of the chemical bond and the structure of molecules and crystals* (Cornell University Press, Ithaca (New York), 1993), 3rd ed., ISBN 0-8014-0333-2.

[10] S. Scheiner, *Hydrogen bonding—A theoretical perspective* (Oxford University Press, New York, Oxford, 1997), ISBN 0-19-509011-X.

[11] D. Hadži, ed., *Theoretical treatments of hydrogen bonding* (John Wiley & Sons, Chichester, New York, 1997), ISBN 0-471-97395-5.

[12] A. Karpfen, in *Adv. Chem. Phys.*, edited by I. Prigogine and S. A. Rice (John Wiley & Sons, New York, 2002), vol. 123, pp. 469–510.

[13] A. Blumen and C. Merkel, Solid State Commun. **20**, 755 (1976).

[14] A. Blumen and C. Merkel, phys. stat. sol. (b) **83**, 425 (1977).

[15] A. Blumen and C. Merkel, Chem. Phys. Lett. **45**, 47 (1977).

[16] C.-M. Liegener and J. J. Ladik, Phys. Rev. B **35**, 6403 (1987).

[17] S. Berski and Z. Latajka, J. Mol. Struct. (Theochem) **389**, 147 (1997).

[18] S. Berski and Z. Latajka, Polish J. Chem. **72**, 1540 (1998).

[19] C. Buth and B. Paulus, Chem. Phys. Lett. **398**, 44 (2004), arXiv:cond-mat/0408243.

[20] C. Buth, Dissertation, Technische Universität Dresden, 01062 Dresden, Germany (2005), nbn-resolving.de/urn:nbn:de:swb:14-1132580113554-34509.

[21] C. Buth and B. Paulus (2006), (unpublished), arXiv:cond-mat/0601470.

[22] A. Zunger, J. Chem. Phys. **63**, 1713 (1975).

[23] L. S. Cederbaum and W. Domcke, in *Adv. Chem. Phys.*, edited by I. Prigogine and S. A. Rice (John Wiley & Sons, New York, 1977), vol. 36, pp. 205–344.

[24] W. von Niessen, J. Schirmer, and L. S. Cederbaum, Comp. Phys. Rep. **1**, 57 (1984).

[25] J. J. Ladik, *Quantum theory of polymers as solids* (Plenum Press, New York, London, 1988), ISBN 0-306-42434-7.

[26] J. J. Ladik, Phys. Rep. **313**, 171 (1999).

[27] A. Shukla, M. Dolg, H. Stoll, and P. Fulde, Chem. Phys. Lett. **262**, 213 (1996).

[28] A. Shukla, M. Dolg, P. Fulde, and H. Stoll, Phys. Rev. B **57**, 1471 (1998).

[29] C. Buth (2006), (unpublished).

[30] C. Buth, U. Birkenheuer, M. Albrecht, and P. Fulde, Phys. Rev. B **72**, 195107 (2005), arXiv:cond-mat/0409078.

[31] J. Schirmer, Phys. Rev. A **26**, 2395 (1982).

[32] J. Schirmer, L. S. Cederbaum, and O. Walter, Phys. Rev. A **28**, 1237 (1983).

[33] M. S. Deleuze, Int. J. Quantum Chem. **93**, 191 (2003).

[34] L. S. Cederbaum, W. Domcke, J. Schirmer, and W. von Niessen, in *Adv. Chem. Phys.*, edited by I. Prigogine and S. A. Rice (John Wiley & Sons, New York, 1986), vol. 65, pp. 115–159.

[35] C. Buth, R. Santra, and L. S. Cederbaum, J. Chem. Phys. **119**, 7763 (2003), arXiv:physics/0306123.

[36] P. Fulde, *Electron correlations in molecules and solids*, vol. 100 of *Springer series in solid-state sciences* (Springer,

Berlin, 1995), 3rd ed., ISBN 3-540-59364-0.

[37] P. Fulde, Adv. Phys. **51**, 909 (2002).

[38] C. Buth, CO-ADC *user's manual*, Max-Planck-Institut für Physik komplexer Systeme, Nöthnitzer Straße 38, 01187 Dresden, Germany (2004), with contributions by Martin Albrecht, Hans-Dieter Meyer, and Thomas Sommerfeld, Version 1.0.0, planet.pks.mpg.de/trac/co-adc.

[39] C. Pisani, R. Dosevi, and C. Roetti, *Hartree-Fock ab initio treatment of crystalline systems*, vol. 48 of *Lecture notes in chemistry* (Springer, Berlin, Heidelberg, 1988), ISBN 3-540-19317-0.

[40] J. Callaway, *Quantum theory of the solid state* (Academic Press, Boston, 1991), 2nd ed., ISBN 0-12-155203-9.

[41] C. Pisani, ed., *Quantum-mechanical ab initio calculation of the properties of crystalline materials*, vol. 67 of *Lecture notes in chemistry* (Springer, Berlin, Heidelberg, 1996), ISBN 3-540-61645-4.

[42] A. Szabo and N. S. Ostlund, *Modern quantum chemistry: Introduction to advanced electronic structure theory* (McGraw-Hill, New York, 1989), 1st, revised ed., ISBN 0-486-69186-1.

[43] R. McWeeny, *Methods of molecular quantum mechanics* (Academic Press, London, 1992), 2nd ed., ISBN 0-12-486551-8.

[44] T. Helgaker, P. Jørgensen, and J. Olsen, *Molecular electronic structure theory* (John Wiley & Sons, Chichester, New York, 2000), ISBN 0-471-96755-6.

[45] R. D. Mattuck, *A guide to Feynman diagrams in the many-body problem* (McGraw-Hill, New York, 1976), 2nd ed., ISBN 0-07-040954-4.

[46] A. L. Fetter and J. D. Walecka, *Quantum theory of many-particle systems*, International series in pure and applied physics, edited by Leonard I. Schiff (McGraw-Hill, New York, 1971).

[47] E. K. U. Gross, E. Runge, and O. Heinonen, *Many-particle theory* (Adam Hilger, Bristol, 1991), ISBN 0-7503-0155-4.

[48] W. von Niessen, P. Tomasello, J. Schirmer, L. S. Cederbaum, R. Cambi, F. Tarantelli, and A. Sgamellotti, J. Chem. Phys. **92**, 4331 (1992).

[49] J. Schirmer and G. Angonoa, J. Chem. Phys. **91**, 1754 (1989).

[50] H.-G. Weikert, H.-D. Meyer, L. S. Cederbaum, and F. Tarantelli, J. Chem. Phys. **104**, 7122 (1996).

[51] T. Sommerfeld and H.-D. Meyer (2004), private communication.

[52] H.-D. Meyer and S. Pal, J. Chem. Phys. **91**, 6195 (1989).

[53] T. Sommerfeld and F. Tarantelli, J. Chem. Phys. **112**, 2106 (2000).

[54] K. P. Huber and G. H. Herzberg, *Molecular spectra and molecular structure. IV. Constants of diatomic molecules* (Van Nostrand-Reinhold, New York, 1979).

[55] N. Wiberg, A. F. Holleman, and E. Wiberg, *Inorganic chemistry* (Academic Press, New York, 2001), ISBN 0-123-52651-5.

[56] T. H. Dunning, Jr., J. Chem. Phys. **90**, 1007 (1989).

[57] D. E. Woon and T. H. Dunning, Jr., J. Chem. Phys. **98**, 1358 (1993).

[58] Basis sets were obtained from the Extensible Computational Chemistry Environment Basis Set Database, Version 02/25/04, as developed and distributed by the Molecular Science Computing Facility, Environmental and Molecular Sciences Laboratory which is part of the Pacific Northwest Laboratory, P.O. Box 999, Richland, Washington 99352, USA, and funded by the U.S. Department of Energy. The Pacific Northwest Laboratory is a multi-program laboratory operated by Battelle Memorial Institute for the U.S. Department of Energy under contract DE-AC06-76RLO 1830. Contact David Feller or Karen Schuchardt for further information.

[59] M. Albrecht (2004), private communication.

[60] P. Pulay, Chem. Phys. Lett. **100**, 151 (1983).

[61] S. Saebø and P. Pulay, Annu. Rev. Phys. Chem. **44**, 213 (1993).

[62] C. Hampel and H.-J. Werner, J. Chem. Phys. **104**, 6286 (1996).

[63] P. Knowles, M. Schütz, and H.-J. Werner, in *Modern methods and algorithms of quantum chemistry*, edited by J. Grotendorst (John von Neumann Institute for Computing, Jülich, 2000), vol. 3 of *NIC series*, pp. 97–179, ISBN 3-00-005834-6, www.fz-juelich.de/nic-series.

[64] S. Feuerbacher, T. Sommerfeld, R. Santra, and L. S. Cederbaum, J. Chem. Phys. **118**, 6188 (2003).

[65] A. B. Trofimov and J. Schirmer, J. Chem. Phys. **123**, 144115 (2005).

[66] M. Albrecht, P. Fulde, and H. Stoll, Chem. Phys. Lett. **319**, 355 (2000).

[67] V. Bezugly and U. Birkenheuer, Chem. Phys. Lett. **399**, 57 (2004), arXiv:cond-mat/0407382.

[68] J. Gräfenstein, H. Stoll, and P. Fulde, Chem. Phys. Lett. **215**, 611 (1993).

[69] J. Gräfenstein, H. Stoll, and P. Fulde, Phys. Rev. B **55**, 13588 (1997).

[70] C. Buth, R. Santra, and L. S. Cederbaum, J. Chem. Phys. **119**, 10575 (2003), arXiv:physics/0303100.

[71] J. Zobeley, L. S. Cederbaum, and F. Tarantelli, J. Chem. Phys. **108**, 9737 (1998).

[72] In Refs. 19,20, the cc-pVDZ basis set[56,57,58] was found to yield rather inaccurate ground-state binding energies of $(HF)_\infty$ and $(HCl)_\infty$ chains; they deviated in both cases by $\approx 0.05\,eV$ from the best value for the binding energy [Tab. 4 of Ref. 19]. In this study, however, such accuracy of the energy levels would be very good. By these numbers, I do not want at all to imply that the computations presented here are that accurate but rather indicate the significantly lowered demands to the quality of the basis set. The error between the results from ADC(2,2) computations and other methods in Tabs. I and II is somewhat larger than the basis set error for the ground-state binding energy.

[73] The intermediate overcompleteness of the virtual space representation is inherent to the projected atomic orbital theory. It is resolved in the WANNIER program[27,28] following Hampel and Werner[62,63] by removing the projected atomic orbitals which correspond to the smallest eigenvalues of the overlap matrix formed in the origin cell.[20,59]

[74] This observation can be compared to studies of the ionization spectra of the xenon fluorides where a shift of the inner valence (and core) IPs to lower energies is observed with increasing number of fluorine ligands. There it is traced back to the fact that the addition of fluorine atoms leads to a reduced screening of the nuclear charge of the xenon atom.[35]

[75] As all calculations with WANNIER[27,28] and CO-ADC[38] are performed without enforcing the rod group symmetry of the chains explicitly in the equations, a tiny artificial splitting of the energy levels occurs at the X-point due to a minute breaking of the symmetry. I remove it by computing the arithmetic mean between pairs of should-be degen-

erate energy levels in Tabs. III and IV.

[76] Due to the fact that the pseudocanonical Wannier orbitals are delocalized over the unit cell,[20,27,28,30] the entire cell has to be treated as the smallest unit for configuration selection. Hence, the application of the very fine grained selection criterion of Refs. 20,30 is not sensible here.